Chapter 6

Passive Modelocking

As we have seen in chapter 5 the pulse width in an actively modelocked laser is inverse proportional to the fourth root of the curvature in the loss modulation. In active modelocking one is limited to the speed of electronic signal generators. Therefore, this curvature can never be very strong. However, if the pulse can modulate the absorption on its own, the curvature of the absorption modulationcan become large, or in other words the net gain window generated by the pulse can be as short as the pulse itself. In this case, the net gain window shortens with the pulse. Therefore, passively modelocked lasers can generate much shorter pulses than actively modelocked lasers.

However, a suitable saturable absorber is required for passive modelocking. Depending on the ratio between saturable absorber recovery time and final pulse width, one may distinguish between the regimes of operation shown in Figure 6.1, which depicts the final steady state pulse formation process. In a solid state laser with intracavity pulse energies much lower than the saturation energy of the gain medium, gain saturation can be neglected. Then a fast saturable absorber must be present that opens and closes the net gain window generated by the pulse immediately before and after the pulse. This modelocking principle is called fast saturable absorber modelocking, see Figure 6.1 a).

In semiconductor and dye lasers usually the intracavity pulse energy exceeds the saturation energy of the gain medium and so the the gain medium undergoes saturation. A short net gain window can still be created, almost independent of the recovery time of the gain, if a similar but unpumped medium is introduced into the cavity acting as an absorber with a somewhat lower saturation energy then the gain medium. For example, this can be

Figure 6.1: Pulse-shaping and stabilization mechanisms owing to gain and loss dynamics in passively mode-locked lasers: (a) using only a fast saturable absorber; (b) using a combination of gain and loss saturation; (c) using a saturable absorber with a finite relaxation time and soliton formation.

arranged for by stronger focusing in the absorber medium than in the gain medium. Then the absorber bleaches first and opens a net gain window, that is closed by the pulse itself by bleaching the gain somewhat later, see Figure 6.1 b). This principle of modelocking is called slow-saturable absorber modelocking.

When modelocking of picosecond and femtosecond lasers with semiconductor saturable absorbers has been developed it became obvious that even with rather slow absorbers, showing recovery times of a few picoseconds, one was able to generate sub-picosecond pulses resulting in a significant net gain window after the pulse, see Figure 6.1 c). From our investigation of active modelocking in the presence of soliton formation, we can expect that such a situation may still be stable up to a certain limit in the presence of strong soliton formation. This is the case and this modelocking regime is called soliton modelocking, since solitary pulse formation due to SPM and GDD shapes the pulse to a stable sech-shape despite the open net gain window following the pulse.

6.1 Slow Saturable Absorber Mode Locking

Due to the small cross section for stimulated emission in solid state lasers, typical intracavity pulse energies are much smaller than the saturation energy of the gain. Therefore, we neglected the effect of gain saturation due to one pulse sofar, the gain only saturates with the average power. However, there are gain media which have large gain cross sections like semiconductors and dyes, see Table 4.1, and typical intracavity pulse energies may become large enough to saturate the gain considerably in a single pass. In fact, it is this effect, which made the mode-locked dye laser so sucessful. The model for the slow saturable absorber mode locking has to take into account the change of gain in the passage of one pulse [1, 2]. In the following, we consider a modelocked laser, that experiences in one round-trip a saturable gain and a slow saturable absorber. In the dye laser, both media are dyes with different saturation intensities or with different focusing into the dye jets so that gain and loss may show different saturation energies. The relaxation equation of the gain, in the limit of a pulse short compared with its relaxation time, can be approximated by

$$\frac{dg}{dt} = -g\frac{|A(t)|^2}{E_L} \tag{6.1}$$

The coefficient E_L is the saturation energy of the gain. Integration of the equation shows, that the gain saturates with the pulse energy $E(t)$

$$E(t) = \int_{-T_{R/2}}^{t} dt|A(t)|^2 \tag{6.2}$$

when passing the gain

$$g(t) = g_i \exp\left[-E(t)/E_L\right] \tag{6.3}$$

where g_i is the initial small signal gain just before the arrival of the pulse. A similar equation holds for the loss of the saturable absorber whose response (loss) is represented by $q(t)$

$$q(t) = q_0 \exp\left[-E(t)/E_A\right] \tag{6.4}$$

where E_A is the saturation energy of the saturable absorber. If the background loss is denoted by l, the master equation of mode-locking becomes

$$\begin{aligned} \frac{1}{T_R}\frac{\partial}{\partial T}A &= [g_i\left(\exp\left(-E(t)/E_L\right)\right)A - lA - \\ &\quad q_0\exp\left(-E(t)/E_A\right)]A + \tfrac{1}{\Omega_f^2}\tfrac{\partial^2}{\partial t^2}A \end{aligned} \tag{6.5}$$

Here, we have replaced the filtering action of the gain $D_g = \frac{1}{\Omega_f^2}$ as produced by a separate fixed filter. An analytic solution to this integro-differential equation can be obtained with one approximation: the exponentials are expanded to second order. This is legitimate if the population depletions of the gain and saturable absorber media are not excessive. Consider one of these expansions:

$$q_0\exp\left(-E(t)/E_A\right) \approx q_0\left[1-\left(E(t)/E_A\right)+\frac{1}{2}\left(E(t)/E_A\right)^2\right]. \tag{6.6}$$

We only consider the saturable gain and loss and the finite gain bandwidth. Than the master equation is given by

$$T_R\frac{\partial A(T,t)}{\partial T} = \left[g(t)-q(t)-l+D_f\frac{\partial^2}{\partial t^2}\right]A(T,t). \tag{6.7}$$

The filter dispersion, $D_f = 1/\Omega_f^2$, effectively models the finite bandwidth of the laser, that might not be only due to the finite gain bandwidth, but includes all bandwidth limiting effects in a parabolic approximation. Suppose the pulse is a symmetric function of time. Then the first power of the integral gives an antisymmetric function of time, its square is symmetric. An antisymmetric function acting on the pulse $A(t)$ causes a displacement. Hence, the steady state solution does not yield zero for the change per pass, the derivative $\frac{1}{T_R}\frac{\partial A}{\partial T}$ must be equated to a time shift Δt of the pulse. When this is done one can confirm easily that $A(t) = A_o\ \mathrm{sech}(t/\tau)$ is a solution of (6.6) with constraints on its coefficients. Thus we, are looking for a "steady state" solution $A(t,T) = A_o\ \mathrm{sech}(\frac{t}{\tau}+\alpha\frac{T}{T_R})$.Note, that α is the fraction of the pulsewidth, the pulse is shifted in each round-trip due to the shaping by loss and gain. The constraints on its coefficients can be easily found using

the following relations for the sech-pulse

$$E(t) = \int_{-T_{R/2}}^{t} dt|A(t)|^2 = \frac{W}{2}\left(1+\tanh(\frac{t}{\tau}+\alpha\frac{T}{T_R})\right) \quad (6.8)$$

$$E(t)^2 = \left(\frac{W}{2}\right)^2\left(2+2\tanh(\frac{t}{\tau}+\alpha\frac{T}{T_R})-\mathrm{sech}^2(\frac{t}{\tau}+\alpha\frac{T}{T_R})\right) \quad (6.9)$$

$$T_R\frac{\partial}{\partial T}A(t,T) = -\alpha\tanh(\frac{t}{\tau}+\alpha\frac{T}{T_R})A(t,T) \quad (6.10)$$

$$\frac{1}{\Omega_f^2}\frac{\partial^2}{\partial t^2}A(t,T) = \frac{1}{\Omega_f^2\tau^2}\left(1-2\mathrm{sech}^2(\frac{t}{\tau}+\alpha\frac{T}{T_R})\right)A(t,T), \quad (6.11)$$

substituing them into the master equation (6.5) and collecting the coefficients in front of the different temporal functions. The constant term gives the necessary small signal gain

$$g_i\left[1-\frac{W}{2E_L}+\left(\frac{W}{2E_L}\right)^2\right] = l+q_0\left[1-\frac{W}{2E_A}+\left(\frac{W}{2E_A}\right)^2\right]-\frac{1}{\Omega_f^2\tau^2}. \quad (6.12)$$

The constant in front of the odd tanh −function delivers the timing shift per round-trip

$$\alpha = \frac{\Delta t}{\tau} = g_i\left[\frac{W}{2E_L}-\left(\frac{W}{2E_L}\right)^2\right]-q_0\left[\frac{W}{2E_A}-\left(\frac{W}{2E_A}\right)^2\right]. \quad (6.13)$$

And finally the constant in front of the sech^2-function determines the pulsewidth

$$\frac{1}{\tau^2} = \frac{\Omega_f^2W^2}{8}\left(\frac{q_0}{E_A^2}-\frac{g_i}{E_L^2}\right) \quad (6.14)$$

These equations have important implications. Consider first the equation for the inverse pulsewidth, (6.14). In order to get a real solution, the right hand side has to be positive. This implies that $q_0/E_A^2 > g_i/E_L^2$. The saturable absorber must saturate more easily, and, therefore more strongly, than the gain medium in order to open a net window of gain (Figure 6.2).

This was accomplished in a dye laser system by stronger focusing into the saturable absorber-dye jet (Reducing the saturation energy for the saturable absorber) than into the gain-dye jet (which was inverted, i.e. optically

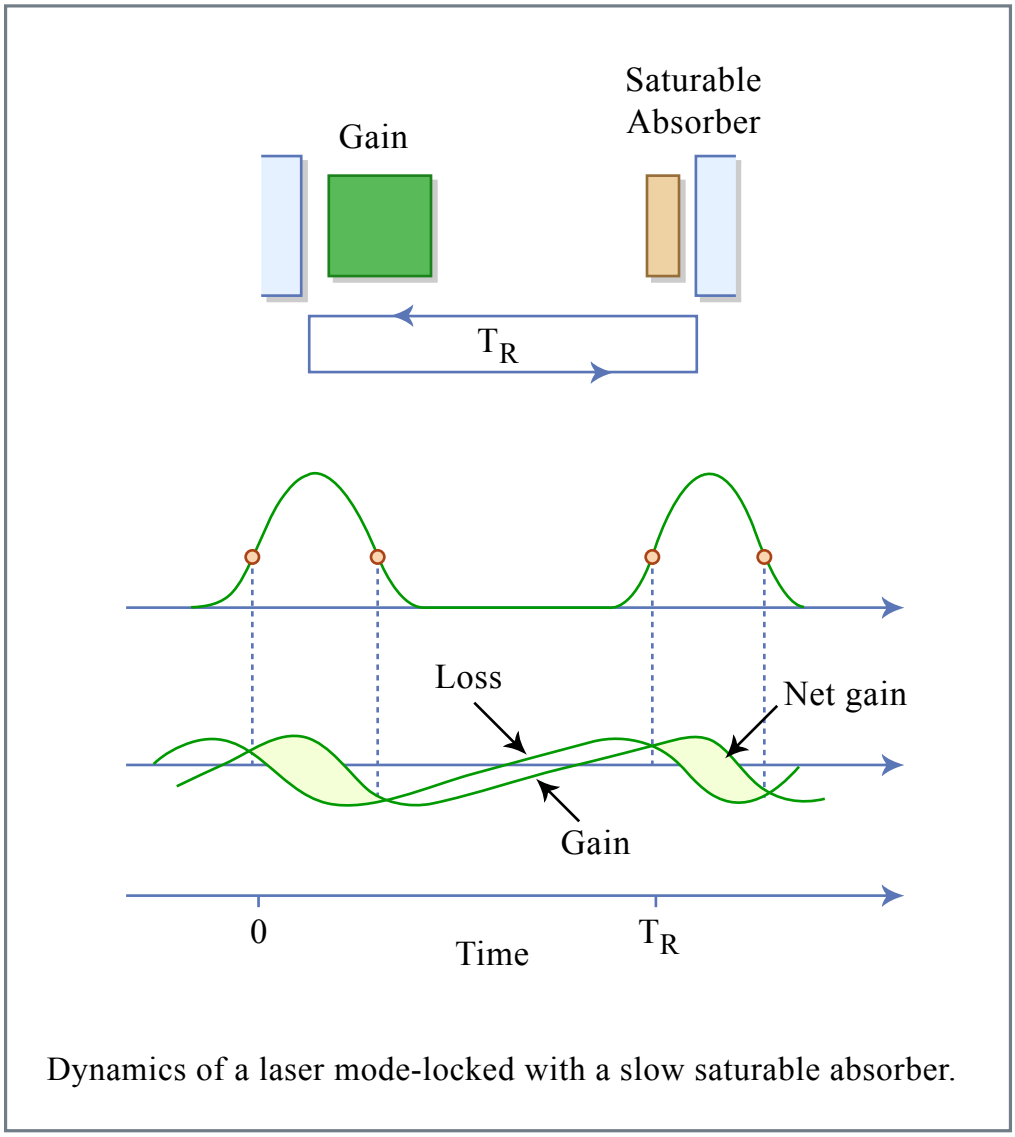

Figure 6.2: Dynamics of a laser mode-locked with a slow saturable absorber.

Figure by MIT OCW.

pumped). Equation (6.12) makes a statement about the net gain before passage of the pulse. The net gain before passage of the pulse is

$$\begin{aligned} g_i - q_0 - l &= -\frac{1}{\Omega_f^2 \tau^2} + g_i \left[\frac{W}{2E_L} - \left(\frac{W}{2E_L} \right)^2 \right] \\ &\quad -q_0 \left[\frac{W}{2E_A} - \left(\frac{W}{2E_A} \right)^2 \right]. \end{aligned} \tag{6.15}$$

Using condition (6.14) this can be expressed as

$$g_i - q_0 - l = g_i \left[\frac{W}{2E_L} \right] - q_0 \left[\frac{W}{2E_A} \right] + \frac{1}{\Omega_f^2 \tau^2} \ . \tag{6.16}$$

This gain is negative since the effect of the saturable absorber is larger than that of the gain. Since the pulse has the same exponential tail after passage as before, one concludes that the net gain after passage of the pulse is the same as before passage and thus also negative. The pulse is stable against noise build-up both in its front and its back. This principle works if the ratio between the saturation energies for the saturable absorber and gain $\chi_P = E_A/E_P$ is very small. Then the shortest pulsewidth achievable with a given system is

$$\tau = \frac{4}{\sqrt{q_0}\Omega_f} \frac{E_A}{W} > \frac{2}{\sqrt{q_0}\Omega_f}. \tag{6.17}$$

The greater sign comes from the fact that our theory is based on the expansion of the exponentials, which is only true for $\frac{W}{2E_A} < 1$. If the filter dispersion $1/\Omega_f^2$ that determines the bandwidth of the system is again replaced by an average gain dispersion g/Ω_g^2 and assuming $g = q_0$. Note that the modelocking principle of the dye laser is a very faszinating one due to the fact that actually non of the elements in the system is fast. It is the interplay between two media that opens a short window in time on the scale of femtoseconds. The media themselves just have to be fast enough to recover completely between one round trip, i.e. on a nanosecond timescale.

Over the last fifteen years, the dye laser has been largely replaced by solid state lasers, which offer even more bandwidth than dyes and are on top of that much easier to handle because they do not show degradation over time. With it came the need for a different mode locking principle, since the saturation energy of these broadband solid-state laser media are much higher

than the typical intracavity pulse energies. The absorber has to open and close the net gain window.

6.2 Fast Saturable Absorber Mode Locking

The dynamics of a laser modelocked with a fast saturable absorber is again covered by the master equation (5.21) [3]. Now, the losses q react instantly on the intensity or power $P(t) = |A(t)|^2$ of the field

$$q(A) = \frac{q_0}{1 + \frac{|A|^2}{P_A}}, \tag{6.18}$$

where P_A is the saturation power of the absorber. There is no analytic solution of the master equation (5.21) with the absorber response (6.18). Therefore, we make expansions on the absorber response to get analytic insight. If the absorber is not saturated, we can expand the response (6.18) for small intensities

$$q(A) = q_0 - \gamma |A|^2, \tag{6.19}$$

with the saturable absorber modulation coefficient $\gamma = q_0/P_A$. The constant nonsaturated loss q_0 can be absorbed in the losses $l_0 = l + q_0$. The resulting master equation is, see also Fig. 6.3

$$T_R \frac{\partial A(T,t)}{\partial T} = \left[g - l_0 + D_f \frac{\partial^2}{\partial t^2} + \gamma |A|^2 + j D_2 \frac{\partial^2}{\partial t^2} - j\delta |A|^2 \right] A(T,t). \tag{6.20}$$

Figure 6.3: Schematic representation of the master equation for a passively modelocked laser with a fast saturable absorber.

Eq. (6.20) is a generalized Ginzburg-Landau equation well known from superconductivity with a rather complex solution manifold.

6.2.1 Without GDD and SPM

We consider first the situation without SPM and GDD, i.e. $D_2{=}\delta = 0$

$$T_R \frac{\partial A(T,t)}{\partial T} = \left[g - l_0 + D_f \frac{\partial^2}{\partial t^2} + \gamma |A|^2 \right] A(T,t). \tag{6.21}$$

Up to the imaginary unit, this equation is still very similar to the NSE. To find the final pulse shape and width, we look for the stationary solution

$$T_R \frac{\partial A_s(T,t)}{\partial T} = 0.$$

Since the equation is similar to the NSE, we try the following ansatz

$$A_s(T,t) = A_s(t) = A_0 \mathrm{sech}\left(\frac{t}{\tau}\right). \tag{6.22}$$

Note, there is

$$\frac{d}{dx}\text{sech}x = -\tanh x\,\text{sech}x, \tag{6.23}$$

$$\begin{aligned}\frac{d^2}{dx^2}\text{sech}x &= \tanh^2 x\,\text{sech}x - \text{sech}^3 x, \\ &= \left(\text{sech}x - 2\,\text{sech}^3 x\right). \end{aligned} \tag{6.24}$$

Substitution of ansatz (6.22) into the master equation (6.21), assuming steady state, results in

$$\begin{aligned}0 = &\left[(g-l_0) + \frac{D_f}{\tau^2}\left[1 - 2\text{sech}^2\left(\frac{t}{\tau}\right)\right]\right. \\ &\left. +\gamma|A_0|^2\text{sech}^2\left(\frac{t}{\tau}\right)\right]\cdot A_0\text{sech}\left(\frac{t}{\tau}\right). \end{aligned} \tag{6.25}$$

Comparison of the coefficients with the sech- and sech^3-expressions results in the conditions for the pulse peak intensity and pulse width τ and for the saturated gain

$$\frac{D_f}{\tau^2} = \frac{1}{2}\gamma|A_0|^2, \tag{6.26}$$

$$g = l_0 - \frac{D_f}{\tau^2}. \tag{6.27}$$

From Eq.(6.26) and with the pulse energy of a sech pulse, see Eq.(3.8), $W = 2|A_0|^2\tau$,

$$\tau = \frac{4D_f}{\gamma W}. \tag{6.28}$$

Eq. (6.28) is rather similar to the soliton width with the exception that the conservative pulse shaping effects GDD and SPM are replaced by gain dispersion and saturable absorption. The soliton phase shift per roundtrip is replaced by the difference between the saturated gain and loss in Eq.(6.28). It is interesting to have a closer look on how the difference between gain and loss $\frac{D_f}{\tau^2}$ per round-trip comes about. From the master equation (6.21) we can derive an equation of motion for the pulse energy according to

$$T_R\frac{\partial W(T)}{\partial T} = T_R\frac{\partial}{\partial T}\int_{-\infty}^{\infty}|A(T,t)|^2\,dt \tag{6.29}$$

$$= T_R\int_{-\infty}^{\infty}\left[A(T,t)^*\frac{\partial}{\partial T}A(T,t) + c.c.\right]dt \tag{6.30}$$

$$= 2G(g_s,W)W, \tag{6.31}$$

where G is the net energy gain per roundtrip, which vanishes when steady state is reached [3]. Substitution of the master equation into (6.30) with

$$\int_{-\infty}^{\infty} \left(\text{sech}^2 x\right) dx = 2, \tag{6.32}$$

$$\int_{-\infty}^{\infty} \left(\text{sech}^4 x\right) dx = \frac{4}{3}, \tag{6.33}$$

$$-\int_{-\infty}^{\infty} \text{sech}x \frac{d^2}{dx^2} \left(\text{sech}x\right) dx = \int_{-\infty}^{\infty} \left(\frac{d}{dx}\text{sech}x\right)^2 dx = \frac{2}{3}. \tag{6.34}$$

results in

$$G(g_s, W) = g_s - l_0 - \frac{D_f}{3\tau^2} + \frac{2}{3}\gamma|A_0|^2 \tag{6.35}$$

$$= g_s - l_0 + \frac{1}{2}\gamma|A_0|^2 = g_s - l_0 + \frac{D_f}{\tau^2} = 0 \tag{6.36}$$

with the saturated gain

$$g_s(W) = \frac{g_0}{1 + \frac{W}{P_L T_R}} \tag{6.37}$$

Equation (6.36) together with (6.28) determines the pulse energy

$$g_s(W) = \frac{g_0}{1 + \frac{W}{P_L T_R}} = l_0 - \frac{D_f}{\tau^2}$$

$$= l_0 - \frac{(\gamma W)^2}{16 D_g} \tag{6.38}$$

Figure 6.4 shows the time dependent variation of gain and loss in a laser modelocked with a fast saturable absorber on a normalized time scale Here, we assumed that the absorber saturates linearly with intensity up to a maximum value $q_0 = \gamma A_0^2$. If this maximum saturable absorption is completely exploited see Figure 6.5.The minimum pulse width achievable with a given saturable absorption q_0 results from Eq.(6.26)

$$\frac{D_f}{\tau^2} = \frac{q_0}{2}, \tag{6.39}$$

to be

$$\tau = \sqrt{\frac{2}{q_0}} \frac{1}{\Omega_f}. \tag{6.40}$$

Figure 6.4: Gain and loss in a passively modelocked laser using a fast saturable absorber on a normalized time scale $x = t/\tau$. The absorber is assumed to saturate linearly with intensity according to $q(A) = q_0 \left(1 - \frac{|A|^2}{A_0^2}\right)$.

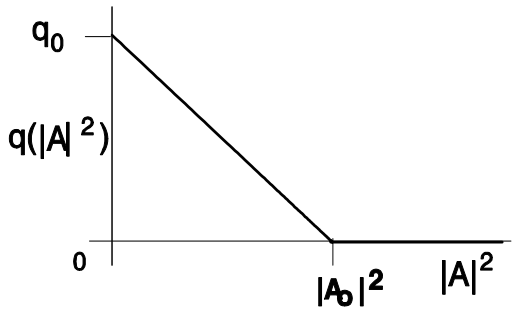

Figure 6.5: Saturation characteristic of an ideal saturable absorber

Note that in contrast to active modelocking, now the achievable pulse width is scaling with the inverse gain bandwidth, which gives much shorter pulses. Figure 6.4 can be interpreted as follows: In steady state, the saturated gain is below loss, by about one half of the exploited saturable loss before and after the pulse. This means, that there is net loss outside the pulse, which keeps the pulse stable against growth of instabilities at the leading and trailing edge of the pulse. If there is stable mode-locked operation, there must be always net loss far away from the pulse, otherwise, a continuous wave signal running at the peak of the gain would experience more gain than the pulse and would break through. From Eq.(6.35) follows, that one third of the exploited saturable loss is used up during saturation of the aborber and actually only one sixth is used to overcome the filter losses due to the finite gain bandwidth. Note, there is a limit to the mimium pulse width, which comes about, because the saturated gain (6.27) is $g_s = l + \frac{1}{2}q_0$ and, therefore, from Eq.(6.40), if we assume that the finite bandwidth of the laser is set by the gain, i.e. $D_f = D_g = \frac{g}{\Omega_g^2}$ we obtain for $q_0 \gg l$

$$\tau_{\min} = \frac{1}{\Omega_g} \tag{6.41}$$

for the linearly saturating absorber model. This corresponds to mode locking over the full bandwidth of the gain medium, since for a sech-shaped pulse, the time-bandwidth product is 0.315, and therefore,

$$\Delta f_{FWHM} = \frac{0.315}{1.76 \cdot \tau_{\min}} = \frac{\Omega_g}{1.76 \cdot \pi}. \tag{6.42}$$

As an example, for Ti:sapphire this corresponds to $\Omega_g = 270$ THz, $\tau_{\min} = 3.7$ fs, $\tau_{FWHM} = 6.5$ fs.

6.2.2 With GDD and SPM

After understanding what happens without GDD and SPM, we look at the solutions of the full master equation (6.20) with GDD and SPM. It turns out, that there exist steady state solutions, which are chirped hyperbolic secant functions [4]

$$A_s(T,t) = A_0 \left(\operatorname{sech}\left(\frac{t}{\tau}\right)\right)^{(1+j\beta)} e^{j\psi T/T_R}, \tag{6.43}$$

$$= A_0 \operatorname{sech}\left(\frac{t}{\tau}\right) \exp\left[j\beta \ln \operatorname{sech}\left(\frac{t}{\tau}\right) + j\psi T/T_R\right]. \tag{6.44}$$

Where ψ is the round-trip phase shift of the pulse, which we have to allow for. Only the intensity of the pulse becomes stationary. There is still a phase-shift per round-trip due to the difference between the group and phase velocity (these effects have been already transformed away) and the nonlinear effects. As in the last section, we can substitute this ansatz into the master equation and compare coefficients. Using the following relations

$$\begin{aligned}
\frac{d}{dx}\left(f(x)^b\right) &= bf(x)^{b-1}\frac{d}{dx}f(x) && (6.45)\\
\frac{d}{dx}\left(\mathrm{sech}x\right)^{(1+j\beta)} &= -\left(1+j\beta\right)\tanh x\left(\mathrm{sech}x\right)^{(1+j\beta)}, && (6.46)\\
\frac{d^2}{dx^2}\left(\mathrm{sech}x\right)^{(1+j\beta)} &= \left((1+j\beta)^2-\left(2+3j\beta-\beta^2\right)\mathrm{sech}^2x\right) && (6.47)\\
& \quad \left(\mathrm{sech}x\right)^{(1+j\beta)}. && (6.48)
\end{aligned}$$

in the master equation and comparing the coefficients to the same functions leads to two complex equations

$$\begin{aligned}
\frac{1}{\tau^2}\left(D_f+jD_2\right)\left(2+3j\beta-\beta^2\right) &= \left(\gamma-j\delta\right)|A_0|^2, && (6.49)\\
l_0-\frac{\left(1+j\beta\right)^2}{\tau^2}\left(D_f+jD_2\right) &= g-j\psi. && (6.50)
\end{aligned}$$

These equations are extensions to Eqs.(6.26) and (6.27) and are equivalent to four real equations for the phase-shift per round-trip ψ, the pulse width τ, the chirp β and the peak power $|A_0|^2$ or pulse energy. The imaginary part of Eq.(6.50) determines the phase-shift only, which is most often not of importance. The real part of Eq.(6.50) gives the saturated gain

$$g = l_0-\frac{1-\beta^2}{\tau^2}D_f+\frac{2\beta D_2}{\tau^2}. \tag{6.51}$$

The real part and imaginary part of Eq.(6.49) give

$$\begin{aligned}
\frac{1}{\tau^2}\left[D_f\left(2-\beta^2\right)-3\beta D_2\right] &= \gamma|A_0|^2, && (6.52)\\
\frac{1}{\tau^2}\left[D_2\left(2-\beta^2\right)+3\beta D_f\right] &= -\delta|A_0|^2. && (6.53)
\end{aligned}$$

We introduce the normalized dispersion, $D_n = D_2/D_f$, and the pulse width of the system without GDD and SPM, i.e. the width of the purely saturable

absorber modelocked system, $\tau_0 = 4D_f/(\gamma W)$. Deviding Eq.(6.53) by (6.52) and introducing the normalized nonlinearity $\delta_n = \delta/\gamma$, we obtain a quadratic equation for the chirp,

$$\frac{D_n\left(2-\beta^2\right)+3\beta}{\left(2-\beta^2\right)-3\beta D_n} = -\delta_n,$$

or after some reodering

$$\frac{3\beta}{2-\beta^2} = \frac{\delta_n + D_n}{-1+\delta_n D_n} \equiv \frac{1}{\chi}. \tag{6.54}$$

Note that χ depends only on the system parameters. Therefore, the chirp is given by

$$\beta = -\frac{3}{2}\chi \pm \sqrt{\left(\frac{3}{2}\chi\right)^2 + 2}. \tag{6.55}$$

Knowing the chirp, we obtain from Eq.(6.52) the pulsewidth

$$\tau = \frac{\tau_0}{2}\left(2-\beta^2-3\beta D_n\right), \tag{6.56}$$

which, with Eq.(6.54), can also be written as

$$\tau = \frac{3\tau_0}{2}\beta\left(\chi - D_n\right) \tag{6.57}$$

In order to be physically meaning full the pulse width has to be a positive number, i.e. the product $\beta\left(\chi - D_n\right)$ has always to be greater than 0, which determines the root in Eq.(6.55)

$$\beta = \begin{cases} -\frac{3}{2}\chi + \sqrt{\left(\frac{3}{2}\chi\right)^2 + 2}, & \text{for} \quad \chi > D_n \\ -\frac{3}{2}\chi - \sqrt{\left(\frac{3}{2}\chi\right)^2 + 2}, & \text{for} \quad \chi < D_n \end{cases}. \tag{6.58}$$

Figure 6.6(a,b and d) shows the resulting chirp, pulse width and nonlinear round-trip phase shift with regard to the system parameters [4][5]. A necessary but not sufficient criterion for the stability of the pulses is, that there must be net loss leading and following the pulse. From Eq.(6.51), we obtain

$$g_s - l_0 = -\frac{1-\beta^2}{\tau^2}D_f + \frac{2\beta D_2}{\tau^2} < 0. \tag{6.59}$$

If we define the stability parameter S

$$S = 1 - \beta^2 - 2\beta D_n > 0, \tag{6.60}$$

S has to be greater than zero, as shown in Figure 6.6 (d).

Image removed due to copyright restrictions.

Please see:
Haus, H. A., J. G. Fujimoto, E. P. Ippen. "Structure for additive pulse modelocking." *Journal of Optical Society of Americas B* 8 (1991): 208.

Figure 6.6: (a) Pulsewidth, (b) Chirp parameter, (c) Net gain following the pulse, which is related to stability. (d) Phase shift per pass. [4]

Figure 6.6 (a-d) indicate that there are essentially three operating regimes. First, without GDD and SPM, the pulses are always stable. Second, if there is strong soliton-like pulse shaping, i.e. $\delta_n \gg 1$ and $-D_n \gg 1$ the chirp is always much smaller than for positive dispersion and the pulses are soliton-like. At last, the pulses are even chirp free, if the condition $\delta_n = -D_n$ is fulfilled. Then the solution is

$$A_s(T,t) = A_0 \left(\operatorname{sech}\left(\frac{t}{\tau}\right)\right) e^{j\psi T/T_R}, \text{ for } \delta_n = -D_n. \tag{6.61}$$

Note, for this discussion we always assumed a positive SPM-coefficient. In this regime we also obtain the shortest pulses directly from the system, which can be a factor 2-3 shorter than by pure saturable absorber modelocking. Note that Figure 6.6 indicates even arbitrarily shorter pulses if the nonlinear index, i.e. δ_n is further increased. However, this is only an artificat of the linear approximation of the saturable absorber, which can now become arbitrarily large, compare (6.18) and (6.19). As we have found from the analysis of the fast saturable absorber model, Figure 6.4, only one sixth of the saturable absorption is used for overcoming the gain filtering. This is so, because the saturable absorber has to shape and stabilize the pulse against breakthrough of cw-radiation. With SPM and GDD this is relaxed. The pulse shaping can be done by SPM and GDD alone, i.e. soliton formation and the absorber only has to stabilize the pulse. But then all of the saturable absorption can be used up for stability, i.e. six times as much, which allows for additional pulse shorteing by a factor of about $\sqrt{6} = 2.5$ in a parbolic filter situation. Note, that for an experimentalist a factor of three is a large number. This tells us that the 6.5 fs limit for Ti:sapphire derived above from the saturable absorber model can be reduced to 2.6 fs including GDD and SPM, which is about one optical cycle of 2.7 fs at a center wavelength of 800nm. At that point all approximations, we have mode so far break down. If the amount of negative dispersion is reduced too much, i.e. the pulses become to short, the absorber cannot keep them stable anymore.

If there is strong positive dispersion, the pulses again become stable and long, but highly chirped. The pulse can then be compressed externally, however not completely to their transform limit, because these are nonlinearly chirped pulses, see Eq.(6.43).

In the case of strong solitonlike pulse shaping, the absorber doesn't have to be really fast, because the pulse is shaped by GDD and SPM and the absorber has only to stabilize the soliton against the continuum. This regime has been called Soliton mode locking.

6.3 Soliton Mode Locking

If strong soliton formation is present in the system, the saturable absorber doesn't have to be fast [6][7][8], see Figure 6.7. The master equation descibing

the mode locking process is given by

$$T_R \frac{\partial A(T,t)}{\partial T} = \left[g - l + (D_f + jD) \frac{\partial^2}{\partial t^2} - j\delta |A(T,t)|^2 - q(T,t) \right] A(T,t). \tag{6.62}$$

The saturable absorber obeys a separate differential equation that describes the absorber response to the pulse in each round trip

$$\frac{\partial q(T,t)}{\partial t} = -\frac{q - q_0}{\tau_A} - \frac{|A(T,t)|^2}{E_A}. \tag{6.63}$$

Where τ_A is the absorber recovery time and E_A the saturation energy. If the soliton shaping effects are much larger than the pulse

Image removed due to copyright restrictions.

Please see:
Kartner, F. X., and U. Keller. "Stabilization of soliton-like pulses with a slow saturable absorber." *Optics Letters* 20 (1990): 16-19.

Figure 6.7: Response of a slow saturable absorber to a soliton-like pulse. The pulse experiences loss during saturation of the absorber and filter losses. The saturated gain is equal to these losses. The loss experienced by the continuum, l_c must be higher than the losses of the soliton to keep the soliton stable.

Figure 6.8: The continuum, that might grow in the opten net gain window following the pulse is spread by dispersion into the regions of high absorption.

shaping due to the filter and the saturable absorber, the steady state pulse will be a soliton and continuum contribution similar to the case of active mode locking with strong soliton formation as discussed in section 5.5

$$A(T,t) = \left(A\,\mathrm{sech}(\frac{t}{\tau}) + a_c(T,t) \right) e^{-j\phi_0 \frac{T}{T_R}} \tag{6.64}$$

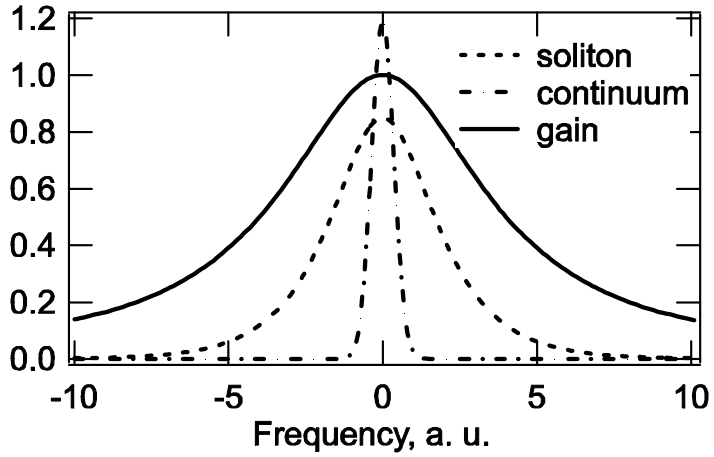

Figure 6.9: Normalized gain, soliton and continuum. The continuum is a long pulse exploiting the peak of the gain

The continuum can be viewed as a long pulse competing with the soliton for the available gain. In the frequency domain, see Figure 6.9, the soliton has a broad spectrum compared to the continuum. Therefore, the continuum experiences the peak of the gain, whereas the soliton spectrum on average experiences less gain. This advantage in gain of the continuum has to be compensated for in the time domain by the saturable absorber response, see Figure 6.8. Whereas for the soliton, there is a balance of the nonlinearity and the dispersion, this is not so for the continuum. Therefore, the continuum is spread by the dispersion into the regions of high absorption. This mechanism has to clean up the gain window following the soliton and caused by the slow recovery of the absorber. As in the case of active modelocking, once the soliton is too short, i.e. a too long net-gain window arises, the loss of the continuum may be lower than the loss of the soliton, see Figure 6.7 and the continuum may break through and destroy the single pulse soliton solution. As a rule of thumb the absorber recovery time can be about 10 times longer than the soliton width. This modelocking principle is especially important for modelocking of lasers with semiconductor saturable absorbers, which show typical absorber recovery times that may range from 100fs-100 ps. Pulses as short as 13fs have been generated with semiconductor saturable absorbers [11]. Figure 6.10 shows the measured spectra from a Ti:sapphire laser modelocked with a saturable absorber for different values for the intracavity dispersion. Lowering the dispersion, increases the bandwidth of the soliton and therefore its loss, while lowering at the same time the loss for the continuum. At some value of the dispersion the laser has to become unstabile by break through of the continuum. In the example shown, this occurs at a dispersion value of about $D = -500fs^2$. The continuum break-through is clearly visible by the additional spectral components showing up at the center of the spectrum. Reducing the dispersion even further might lead again to more stable but complicated spectra related to the formation of higher order solitons. Note the spectra shown are time averaged spectra.

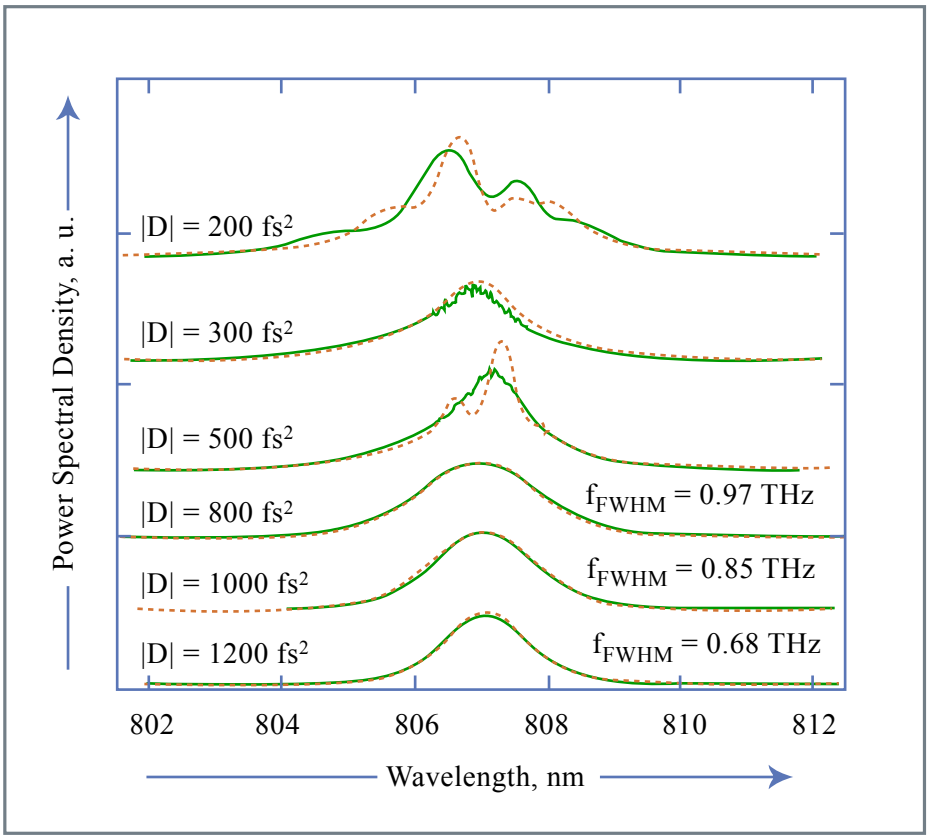

Figure 6.10: Measured (—) and simulated (- - -) spectra from a semiconductor saturable absorber modelocked Ti:sapphire laser for various values of the net intracavity dispersion.

Figure by MIT OCW.

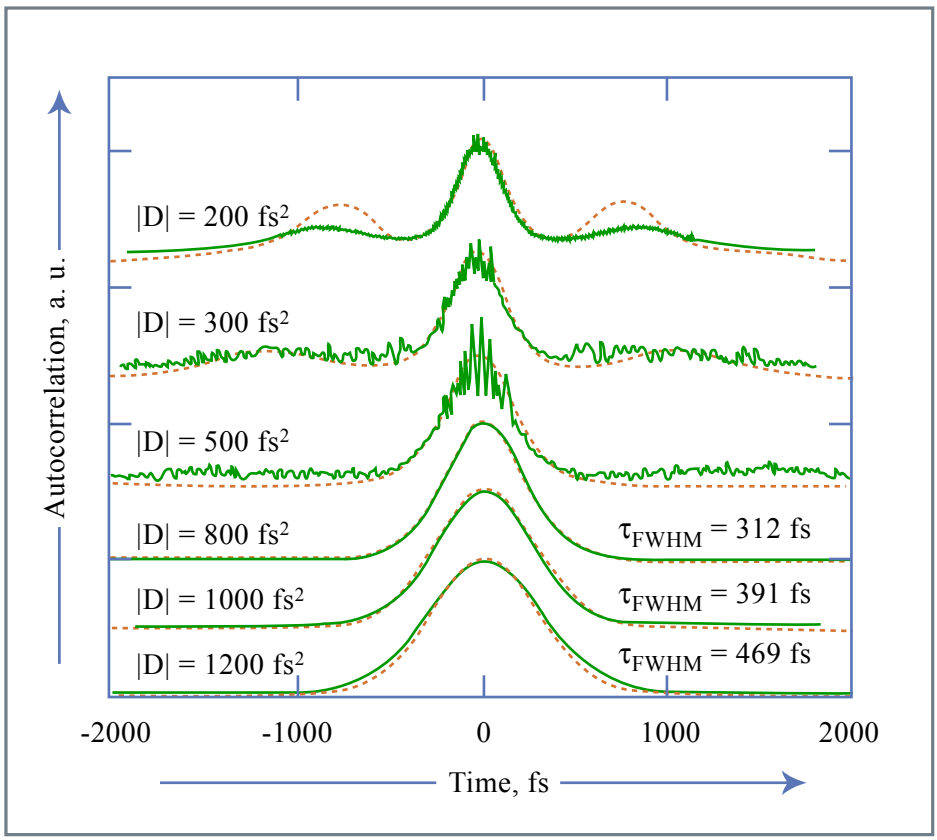

Figure 6.11: Measured (—-) and simulated (- - -) autocorrelations corresponding to the spectra shown in Figure 6.10.

Figure by MIT OCW.

The continuum leads to a background pedestal in the intensity autocorrelation of the emitted pulse, see Figure 6.11. The details of the spectra and autocorrelation may strongly depend on the detailed absorber response.

6.4 Dispersion Managed Soliton Formation

The nonlinear Schrödinger equation describes pulse propagation in a medium with continuously distributed dispersion and self-phase-modulation. For lasers generating pulses as short as 10 fs and below, it was first pointed out by Spielmann et al. that large changes in the pulse occur within one roundtrip and that the ordering of the pulse-shaping elements within the cavity has a major effect on the pulse formation [9]. The discrete action of linear dispersion in the arms of the laser resonator and the discrete, but simultaneous, action of positive SPM and positive GDD in the laser crystal cannot any longer be neglected. The importance of strong dispersion variations for the laser dynamics was first discovered in a fiber laser and called stretched pulse modelocking [11]. The positive dispersion in the Er-doped fiber section of a fiber ring laser was balanced by a negative dispersive passive fiber. The pulse circulating in the ring was stretched and compressed by as much as a factor of 20 in one roundtrip. One consequence of this behavior was a dramatic decrease of the nonlinearity and thus increased stability against the SPM induced instabilities. The sidebands, due to periodic perturbations of the soliton, as discussed in section 3.6, are no longer observed (see Fig. 6.12).

Figure 6.12: Spectra of mode-locked Er-doped fiber lasers operating in the conventional soliton regime, i.e. net negative dispersion and in the stretched pulse mode of operation at almost zero average dispersion [11].

The energy of the output pulses could be increased 100 fold. The minimum pulsewidth was 63 fs, with a bandwdith much broader than the erbium gain bandwidth [12]. Figure 6.12 also shows the spectral enhancement of the fiber laser in the dispersion managed regime. The generation of ultrashort pulses from solid state lasers like Ti:sapphire has progressed over the past decade and led to the generation of pulses as short as 5 fs directly from the laser. At such short pulse lengths the pulse is streched up to a factor of ten when propagating through the laser crystal creating a dispersion managed soliton [10]. The spectra generated with these lasers are not of simple shape for many reasons. Here, we want to consider the impact on the spectral shape and laser dynamcis due to dispersion managed soliton formation.

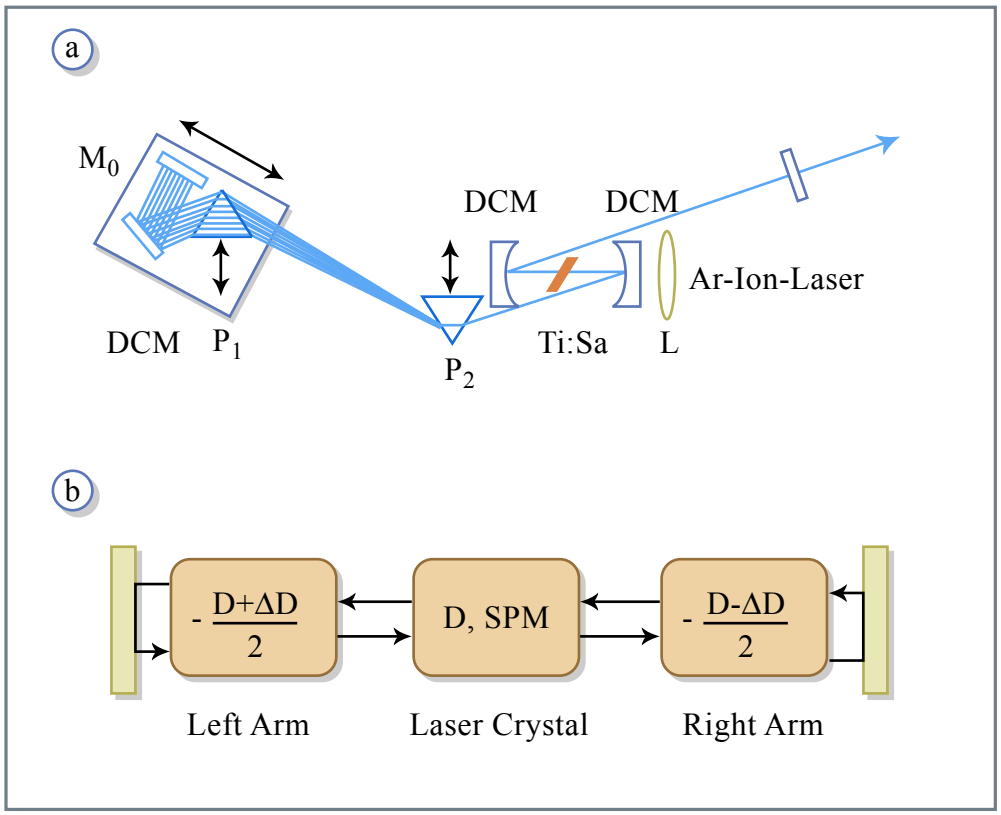

Figure 6.13: (a) Schematic of a Kerr-lens mode-locked Ti:sapphire laser: P's, prisms; L, lens; DCM's, double-chirped mirror; TiSa, Ti:sapphire. (b) Correspondence with dispersion-managed fiber transmission.

Figure by MIT OCW.

A mode-locked laser producing ultrashort pulses consists at least of a gain

medium (Ti:sapphire crystal) and dispersion balancing components (mirrors, prism pairs), see Fig. 6.13 a. The system can be decomposed into the resonator arms and the crystal, see Fig. 6.13 b. To achieve ultrashort pulses, the dispersion-balancing components should produce near-zero net dispersion while the dispersion element(s) individually produce significant group delay over the broad bandwidth of the laser pulse. This fact suggests an analogy with dispersion-managed pulse propagation along a dispersion-managed fiber transmission link [14]. A system with sufficient variation of dispersion can support solitary waves. One can show that the Kerr nonlinearity produces a self-consistent nonlinear scattering potential that permits formation of a perodic solution with a simple phase factor in a system with zero net dispersion. The pulses are analogous to solitons in that they are self-consistent solutions of the Hamiltonian (lossless) problem as the conventional solitons discussed above. But they are not secant hyperbolic in shape. Figure 6.14 shows a numerical simulation of a self-consistent solution of the Hamiltonian pulse-propagation problem in a linear medium of negative dispersion and subsequent propagation in a nonlinear medium of positive dispersion and positive self-phase modulation, following the equation

$$\frac{\partial}{\partial z}A(z,t) = jD(z)\frac{\partial^2}{\partial t^2}A(z,t) - j\delta(z)|A|^2A(z,t) \tag{6.65}$$

In Fig. 6.15 the steady state intensity profiles are shown at the center of the negative dispersion segment over 1000 roundtrips. It is clear that the solution repeats itself from period to period, i.e. there is a new solitary wave that solves the piecewise nonlinear Schroedinger equation 6.65, dispersion managed soliton. In contrast to the conventional soliton the dispersion mangaged soliton of equation 6.65 (with no SAM and no filtering) resemble Gaussian pulses down to about -10 dB from the peak, but then show rather complicated structure, see Fig. 6.15.The dispersion map $D(z)$ used is shown as an inset in Figure 6.14. One can additionally include saturable gain, Lorentzian gain filtering, and a fast saturable absorber. Figure 6.14 shows the behavior in one period (one round trip through the resonator) including these effects. The response of the absorber is $q(A) = q_o/(1+|A|^2/P_A)$, with $q_o = 0.01/\text{mm}$ and $P_A = 1$ MW. The bandwidth-limited gain is modeled by the Lorentzian profile with gain bandwidth $2\pi \times 43$ THz. The filtering and saturable absorption reduce the spectral and temporal side lobes of the Hamiltonian problem. As can be inferred from Fig. 6.14, the steady state pulse formation can be understood in the following way. By symmetry the pulses are chirp free in

Figure 6.14: Pulse shaping in one round trip. The negative segment has no nonlinearity.

the middle of the dispersion cells. A chirp free pulse starting in the center of the gain crystal, i.e. nonlinear segment is spectrally broadened by the SPM and disperses in time due to the GVD, which generates a rather linear chirp over the pulse. After the pulse is leaving the crystal it experiences negative GVD during propagation through the left or right resonator arm, which is compressing the positively chirped pulse to its transform limit at the end of the arm, where an output coupler can be placed. Back propagation towards the crystal imposes a negative chirp, generating the time reversed solution of the nonliner Schrödinger equation (6.65). Therefore, subsequent propagation in the nonlinear crystal is compressing the pulse spectrally and temporally to its initial shape in the center of the crystal. The spectrum is narrower in the crystal than in the negative-dispersion sections, because it is negatively prechirped before it enters the SPM section and spectral spreading occurs again only after the pulse has been compressed. This result further explains that in a laser with a linear cavity, for which the negative dispersion is located in only one arm of the laser resonator (i.e. in the prism pair and no use of chirped mirrors) the spectrum is widest in the arm that contains the negative dispersion . In a laser with a linear cavity, for which the negative dispersion is equally distributed in both arms of the cavity, the pulse runs

through the dispersion map twice per roundtrip. The pulse is short at each end of the cavity and, most importantly, the pulses are identical in each pass through the crystal, which exploits the saturable absorber action (Kerr-Lens Modelocking in this case, as will be discussed in the next chapter) twice per roundtrip, in contrast to an asymmetric dispersion distribution in the resonator arms. Thus a symmetric dispersion distribution leads to an effective saturable absorption that is twice as strong as an asymmetric dispersion distribution resulting in substantially shorter pulses. Furthermore, the dispersion swing between the negative and positive dispersion sections is only half, which allows for shorter dispersion-managed solitons operating at the same average power level.

Figure 6.15: Simulation of the Hamiltonian problem. Intensity profiles at the center of the negatively dispersive segment are shown for successive roundtrips. The total extent in 1000 roundtrips. $D = D^{(\pm)} = \pm 60$ fs^2/mm, segment of crystal length $L = 2$ mm, $\tau_{\mathrm{FWHM}} = 5.5$ fs, $\delta = 0$ for $D < 0$, $\delta = 1$ (MW mm)$^{-1}$ for $D > 0$. [10]

To further illustrate the efficiency of the dispersion managed soliton formation, we present a series of simulations that start with a linear segment of negative dispersion and a nonlinear segment of positive dispersion of the same magnitude, saturable absorber action, and filtering.

Image removed due to copyright restrictions.

Please see:
Chen, Y., et al. "Dispersion managed mode-locking." *Journal of Optical Society of Americas B* 16 (1999): 1999-2004.

Figure 6.16: Sequence of pulse profiles in the center of the negatively dispersive segment for three magnitudes of SPM. $t_o = 3$ fs, with solid curves (5.5 fs) for $\delta = 1$ (MW mm)$^{-1}$, dashed-dotted curve (7 fs) for $\delta = 0.5$ (MW mm)$^{-1}$, and dashed cuves for no SPM of $\delta = 0$. The dispersion map is of Fig. 6.14. The output coupler loss is 3%.[10]

The dashed curve in Figure 6.16 shows the pulse shape for gain, loss, saturable absorption and gain filtering only. We obtained the other traces by increasing the SPM while keeping the energy fixed through adjustment of the gain. As one can see, increasing the SPM permits shorter pulses. The shortest pulse can be approximately three times shorter than the pulse without SPM. The parameters chosen for the simulations are listed in the figure caption. In this respect, the behavior is similar to the fast saturable absorber case with conventional soliton formation as discussed in the last section.

A major difference in the dispersion managed soliton case is illustrated in Fig. 6.17. The figure shows the parameter ranges for a dispersion-managed soliton system (no gain, no loss, no filtering) that is unbalanced such as to result in the net dispersion that serves as the abscissa of the figure. Each curve gives the locus of energy versus net cavity dispersion for a stretching

ratio $S = LD/\tau^2_{\rm FWHM}$ (or pulse width with fixed crystal length L). One can see that for pulse width longer than 8 fs with crystal length $L = 2$ mm, no solution of finite energy exists in the dispersion managed system for zero or positive net dispersion. Pulses of durations longer than 8 fs require net negative dispersion. Hence one can reach the ultrashort dispersion managed soliton operation at zero net dispersion only by first providing the system with negative dispersion. At the same energy, one can form a shorter pulse by reducing the net dispersion, provided that the 8 fs threshold has been passed. For a fixed dispersion swing $\pm D$, the stretching increases quadratically with the spectral width or the inverse pulse width. Long pulses with no stretching have a sech shape. For stretching ratios of 3-10 the pulses are Gaussian shaped. For even larger stretching ratios the pulse spectra become increasingly more flat topped, as shown in Fig. 6.16.

Figure 6.17: Energy of the pulse in the lossless dispersion-managed system with stretching $S = LD/\tau^2_{\rm FWHM}$ or for a fixed crystal length L and pulsewidth as parameters; $D = 60$ fs^2/mm for Ti:sapphire at 800 nm [10].

To gain insight into the laser dynamics and later on in their noise and tuning behavior, it is advantageous to formulate also a master equation approach for the dispersion managed soliton case [16]. Care has to be taken of the fact that the Kerr-phase shift is produced by a pulse of varying amplitude and width as it circulates around the ring. The Kerr-phase shift for a pulse

of constant width, $\delta|a|^2$ had to be replaced by a phase profile that mimics the average shape of the pulse, weighted by its intensity. Therefore, the SPM action is replaced by

$$\delta|A|^2 = \delta_o|A_o|^2\left(1-\mu\frac{t^2}{\tau^2}\right) \tag{6.66}$$

where A_o is the pulse amplitude at the position of minimum width. The Kerr-phase profile is expanded to second order in t. The coefficient δ_o and μ are evaluated variationally. The saturable absorber action is similarly expanded. Finally, the net intracavity dispersion acting on average on the pulse is replaced by the effective dispersion $D_{\rm net}$ in the resonator within one roundtrip. The master equation becomes

$$\begin{aligned} T_R\frac{\partial}{\partial T}A &= (g-l)A+\left(\frac{1}{\Omega_f^2}+jD_{\rm net}\right)\frac{\partial^2}{\partial t^2}A \\ &\quad +(\gamma_o-j\delta_o)|A_o|^2\left(1-\mu\frac{t^2}{\tau^2}\right)A \end{aligned} \tag{6.67}$$

This equation has Gaussian-pulse solutions. The master equation (6.67) is a patchwork, it is not an ordinary differential equation. The coefficients in the equation depend on the pulse solution and eventually have to be found iteratively. Nevertheless, the equation accounts for the pulse shaping in the system in an analytic fashion. It will allow us to extend the conventional soliton perturbation theory to the case of dispersion managed solitons.

There is one more interesting property of the stretched pulse operation that needs to be emphasized. Dispersion managed solitons may form even when the net dispersion as seen by a linearly propagating pulse is zero or slightly positive. This is a surprising result which was discovered in the study of dispersion managed soliton propagation [14]. It turns out that the stretched pulse changes its spectrum during propagation through the two segments of fiber with opposite dispersion or in the case of a Ti:Sapphire laser in the nonlinear crystal. The spectrum in the segment with normal (positive) dispersion is narrower, than in the segment of anomalous (negative) dispersion, see Figure 6.14. The pulse sees an effective net negative dispersion, provided that the positive $D_{\rm net}$ is not too large. In (6.67) the $D_{\rm net}$ is to be replaced by $D_{\rm eff}$ which can be computed variationally. Thus,

dispersion managed soliton-like solutions can exist even when D_{net} is zero. However, they exist only if the stretching factor is large, see Figure 6.17.

A remarkable property of the dispersion managed solitons is that they do not radiate (generate continuum) even though they propagate in a medium with abrupt dispersion changes. This can be understood by the fact, that the dispersion mangaged soliton is a solution of the underlaying dynamics incorporating already the periodic dispersion variations including the Kerr-effect. This is in contrast to the soliton in a continuously distributed dispersive environment, where periodic variations in dispersion and nonlinearity leads to radiation.

Bibliography

[1] G.H.C. New: "Pulse evolution in mode-locked quasicontinuous lasers," IEEE J. Quantum Electron. **10**, 115-124 (1974)

[2] H. A. Haus, "Theory of Mode Locking with a Slow Saturable Absorber," IEEE J. Quantum Electron. **11**, pp. 736 – 746 (1975).

[3] H. A. Haus, "Theory of modelocking with a fast saturable absorber," J. Appl. Phys. **46**, pp. 3049 – 3058 (1975).

[4] H. A. Haus, J. G. Fujimoto, E. P. Ippen, "Structures for additive pulse modelocking," J. Opt. Soc. of Am. **B 8**, pp. 2068 – 2076 (1991).

[5] E. P. Ippen, "Principles of passive mode locking," Appl. Phys. **B 58**, pp. 159 – 170 (1994).

[6] F. X. Kärtner and U. Keller, "Stabilization of soliton-like pulses with a slow saturable absorber," Opt. Lett. **20**, 16 – 19 (1995).

[7] F.X. Kärtner, I.D. Jung, U. Keller: TITLE, "Soliton Modelocking with Saturable Absorbers," Special Issue on Ultrafast Electronics, Photonics and Optoelectronics, IEEE J. Sel. Top. Quantum Electron. **2**, 540-556 (1996)

[8] I. D. Jung, F. X. Kärtner, L. R. Brovelli, M. Kamp, U. Keller, "Experimental verification of soliton modelocking using only a slow saturable absorber," Opt. Lett. **20**, pp. 1892 – 1894 (1995).

[9] C. Spielmann, P.F. Curley, T. Brabec, F. Krausz: Ultrabroad-band femtosecond lasers, IEEE J. Quantum Electron. **30**, 1100-1114 (1994).

[10] Y. Chen, F. X. Kärtner, U. Morgner, S. H. Cho, H. A. Haus, J. G. Fujimoto, and E. P. Ippen, "Dispersion managed mode-locking," J. Opt. Soc. Am. B **16**, 1999-2004, 1999.

[11] K. Tamura, E.P. Ippen, H.A. Haus, L.E. Nelson: 77-fs pulse generation from a stretched-pulse mode-locked all-fiber ring laser, Opt. Lett. **18**, 1080-1082 (1993)

[12] K. Tamura, E.P. Ippen, H.A. Haus: Pulse dynamics in stretched-pulse lasers, Appl. Phys. Lett. **67**, 158-160 (1995)

[13] F.X. Kärtner, J. A. d. Au, U. Keller, "Mode-Locking with Slow and Fast Saturable Absorbers-What's the Difference,". Sel. Top. Quantum Electron. **4**, 159 (1998)

[14] J.H.B. Nijhof, N.J. Doran, W. Forysiak, F.M. Knox: Stable soliton-like propagation indispersion-managed system with net anomalous, zero, and nromal dispersion, Electron. Lett. **33**, 1726-1727 (1997)

[15] Y. Chen, H.A. Haus: Dispersion-managed solitons in the net positive dispersion regime, J. Opt. Soc. Am. B **16**, 24-30 (1999)

[16] H.A. Haus, K. Tamura, L.E. Nelson, E.P. Ippen, "Stretched-pulse additive pulse modelocking in fiber ring lasers: theory and experiment," IEEE J. Quantum Electron. **31**, 591-598 (1995)

[17] I. D. Jung, F. X. Kärtner, N. Matuschek, D. H. Sutter, F. Morier-Genoud, Z. Shi, V. Scheuer, M. Tilsch, T. Tschudi, U. Keller, "Semiconductor saturable absorber mirrors supporting sub-10 fs pulses," Appl. Phys. B **65**, pp. 137-150 (1997).